In Vivo Evaluation and Dosimetry of ^{123}I-2-Iodo-D-Phenylalanine, a New Potential Tumor-Specific Tracer for SPECT, in an R1M Rhabdomyosarcoma Athymic Mouse Model

Veerle Kersemans, MSc[1]; Bart Cornelissen, PhD[1,2]; Klaus Bacher, MSc[3]; Ken Kersemans, MSc[4]; Hubert Thierens, PhD[3]; Rudi A. Dierckx, PhD[5]; Bart De Spiegeleer, PhD[1]; Guido Slegers, PhD[1]; and John Mertens, PhD[4]

[1]Laboratory for Radiopharmacy, Universiteit Gent, Gent, Belgium; [2]Laboratory for Molecular Imaging and Targeted Radiotherapy, University of Toronto, Toronto, Ontario, Canada; [3]Department of Medicinal Physics and Radiation Protection, Universiteit Gent, Gent, Belgium; [4]Laboratory for Medical Imaging and Physics, Vrije Universiteit Brussel, Brussels, Belgium; and [5]Division of Nuclear Medicine, Gent University Hospital, Gent, Belgium

Earlier reports described the preferential uptake of D-amino acids in tumor-bearing mice. Moreover, it was shown that in tumor cells in vitro the L-amino acid transporter system seemed to lack stereospecificity. Because of the successful results with $^{123/125}$I-2-iodo-L-phenylalanine, $^{123/125}$I-2-iodo-D-phenylalanine was developed, and its tumor-detecting characteristics were evaluated in vivo. **Methods:** ^{123}I labeling of 2-iodo-D-phenylalanine was performed with a kit formulation by use of Cu^{1+}-assisted nucleophilic exchange. ^{123}I-2-Iodo-D-phenylalanine was evaluated in R1M tumor–bearing athymic mice by dynamic planar imaging (DPI) and dissection. The in vivo stability of the tracer was tested by high-performance liquid chromatography. Tumor tracer retention and tracer contrast were evaluated as a function of time. Two-compartment blood modeling from DPI results and dosimetric calculations from biodistribution results were carried out. Moreover, ^{125}I-2-iodo-D-phenylalanine and ^{18}F-FDG uptake in acute inflammation was investigated. **Results:** ^{123}I-2-Iodo-D-phenylalanine was metabolically stable. Fast, high, and specific tumor retention was observed. Two-compartment modeling confirmed the fast clearance of the tracer through the kidneys to the bladder, as observed by DPI and dissection. Moreover, compared with the L-isomer, ^{123}I-2-iodo-D-phenylalanine demonstrated faster clearance and faster uptake in the peripheral compartment. No accumulation in the abdomen or in the brain was noted. Dosimetry revealed that ^{123}I-2-iodo-D-phenylalanine demonstrated a low radiation burden comparable to those of ^{123}I-2-iodo-L-phenylalanine and ^{123}I-2-iodo-L-tyrosine. Although ^{123}I-2-iodo-D-phenylalanine showed a tumor retention of only 4%, the tumor contrast was increased up to 350% at 19 h after injection. **Conclusion:** ^{123}I-2-Iodo-D-phenylalanine is a promising tracer for diagnostic oncologic imaging because of its high, fast, and specific tumor uptake and fast clearance from blood.

Received Jun. 28, 2005; revision accepted Sep. 14, 2005.

For correspondence or reprints contact: Veerle Kersemans, MSc, 804-925 Bay St., Toronto M5S 3L4, Ontario, Canada.

E-mail address: veerle.kersemans@utoronto.ca

Key Words: ^{123}I-2-iodo-D-phenylalanine; radiolabeled amino acid analog; tumor imaging; D-amino acid; biodistribution

J Nucl Med 2005; 46:2104–2111

At present, more and more interest is being shown in nuclear medicine–based tumor detection by PET and SPECT. The most prominent example is ^{18}F-FDG, which is routinely used for oncologic imaging, but because of its high uptake in the brain and in inflamed tissues, new, more specific oncologic imaging tracers are required (*1*).

Both increased amino acid transport across the cell membrane and an increased rate of protein synthesis are early features of malignant transformation. Amino acid transport of types A and L has been shown to be increased in tumor cells relative to normal tissue, and these transport systems have been the major focus of the development of amino acid tracers for oncologic imaging (*1,2*).

Recently, various radiolabeled L-amino acids were successfully developed to overcome the limitations of ^{18}F-FDG. Moreover, it was demonstrated that the membrane transport of the amino acids reflects the malignancy of the cells and that the incorporation of radiolabeled amino acids into cell proteins is not necessary. The increased amino acid uptake is directly related to the metabolic requirements of the tumor cells (*1,3*). ^{123}I-3-Iodo-α-methyltyrosine is at present the only amino acid tracer routinely used for SPECT but, because of its marked long-term renal accumulation, the development of other radiolabeled amino acid tracers is necessary.

Tamemasa et al. (*4*) suggested the use of D-amino acids as specific tumor-detecting agents. They showed the preferential uptake of some unnatural radiolabeled D-amino acids in

comparison to the L-isoforms in tumor-bearing mice. Moreover, Yanagida et al. (*2*) showed in tumor cells in vitro that system L seems to lack stereospecificity; D-amino acids are transported with a high affinity by L-amino acid transporter (LAT) system subtype 1 (LAT1). The latter, together with the slower excretion of D-amino acids from the tumor cells, could be an important rationale to develop D-amino acids as tumor diagnostic agents (*5*). Moreover, a lower radiation burden is expected from D-amino acids than from the L-isoforms because of their faster clearance from blood as a result of both negligible tissue distribution and incorporation into cell proteins.

Our research group developed $^{123/125}$I-2-iodo-D-phenylalanine and demonstrated its uptake in vitro in an R1M (rhabdomyosarcoma) cell model (*6*). The D-isomer was taken up by LAT1, was overexpressed in many tumors, and accumulated more slowly than, but in the same amounts as, ^{125}I-2-iodo-L-phenylalanine. In this study, we evaluated $^{123/125}$I-2-iodo-D-phenylalanine as a potential new tumor diagnostic agent in vivo in an R1M athymic mouse model by means of dissection and dynamic planar imaging (DPI).

MATERIALS AND METHODS

All of the conventional products mentioned were at least of analytic or clinical grade and were obtained from Sigma-Aldrich. The solvents were of high-performance liquid chromatography (HPLC) quality and were obtained from Chemlab.

Synthesis of 2-Iodo-D-Phenylalanine Precursor

2-Iodo-D-phenylalanine was prepared from 2-bromo-D-phenylalanine (PepTech Corp.) by analogy with 2-iodo-L-phenylalanine as described previously (*3*). Briefly, Cu^{1+}-assisted nucleophilic exchange under the same acidic and reducing conditions was used, and 2-iodo-D-phenylalanine and 2-bromo-D-phenylalanine were recovered separately by reversed-phase HPLC (RP-HPLC). Subsequently, 2-iodo-D-phenylalanine was obtained by evaporation of the mobile phase. Identification and quality control were achieved by liquid chromatography–mass spectroscopy, thin-layer chromatography, and RP-HPLC. Chiral chromatography was used to confirm the chiral purity (*3*).

Radiochemistry

$^{123/125}$I-2-Iodo-D-Phenylalanine. Radioiodination with $^{123}I^-$ (222 MBq; 10–20 μL) or $^{125}I^-$ (37 MBq; 10 μL) (Nordion Europe) of 1.0 mg of 2-iodo-D-phenylalanine was performed by Cu^{1+}-assisted isotopic exchange under acidic and reducing conditions as described previously (*3*). The reaction mixture was rendered isotonic, the pH was adjusted to at least 4, and free $^{123}I^-$ was removed by Ag membrane filtration. Quality control was achieved by RP-HPLC with Sep-Pak C_{18} (Waters, Belgium), and chiral chromatography was used to confirm the chiral purity (*3*).

^{123}I-Iodo-Human Serum Albumin. Radioiodination of human serum albumin (HSA) with ^{123}I (Nordion Europe) was performed by electrophilic substitution with the IODO-GEN (Pierce) technique as described previously (*3*).

In Vivo Experiments

Laboratory Animals. The study protocol was approved by the local ethical committee for animal studies and was within the rules of Belgian legislation. Guidelines of the National Institutes of Health principles of laboratory animal care were followed.

Water and food were freely available during the experimental period.

Male Swiss *nu/nu* mice (n = 30) (Bioservices) were injected subcutaneously in the right flank (armpit region) with 5×10^6 R1M rhabdomyosarcoma cells. Normal tumor growth curves were obtained by use of sliding caliper measurements (*3,7*). For the inflammation model, male NMRI mice (n = 5) (in-house breeding program) were injected in the right biceps brachii with 25 μL of turpentine to create acute inflammation.

During all imaging experiments, the animals were anesthetized by intraperitoneal injection with 75 μL (1.5 mg) of a solution containing pentobarbital at 20 mg/mL (Nembutal [Ceva Santé Animale], 60 mg/mL). For the biodistribution experiments involving dissection, the animals were sacrificed by cervical dislocation without sedation, and the organs of interest were dissected.

$^{123/125}$I-2-Iodo-D-phenylalanine, ^{18}F-FDG, and ^{123}I-iodo-HSA were injected intravenously in the lateral tail vein.

DPI. Imaging was performed as described previously in the planar mode with a γ-camera (GCA-9300A/hg; Toshiba) equipped with a high-resolution parallel-hole collimator (*3*). All experiments were conducted with the same mouse population to limit the number of animals needed.

In order to perform semiquantitative analysis, a syringe with known ^{123}I-2-iodo-D-phenylalanine activity (measured with a calibrated ionization chamber; Capintec CRC-15R [Ramsey]) was used for dose calibration. Syringes containing ^{123}I-2-iodo-D-phenylalanine were counted with the same Capintec chamber before injection. Tracer uptake was expressed as the differential uptake ratio (DUR): (counts in tissue × pixels in total body)/(pixels in tissue × counts in total body). The latter calculation was performed in accordance with the conclusions and recommendations of Boellaard et al. (*8*) and Thie (*9*).

At first, a ^{123}I-iodo-HSA study was performed to measure the relative blood-pool distribution to correct the uptake of ^{123}I-2-iodo-D-phenylalanine in the studied organs for blood-pool activity (*3*).

DPI experiments were started when the tumor reached a volume of 1 cm^3. Immediately after injection of 18.5 MBq of ^{123}I-2-iodo-D-phenylalanine, a dynamic acquisition was performed; this acquisition was followed by a displacement study with L-phenylalanine (200 μL of a solution at 145 mmol/L intravenously) at steady state. Regions of interest (ROIs) were drawn by use of MRI maximum-intensity projection as described previously (*3*). ^{123}I-2-Iodo-D-phenylalanine uptake by tumors was compared with uptake in the contralateral background area, and the ratio of tumor to contralateral background (RTB) was calculated. The significance of displacement of ^{123}I-2-iodo-D-phenylalanine activity by L-phenylalanine was calculated for a 95% confidence interval.

To test the tumor retention of ^{123}I-2-iodo-D-phenylalanine, 3 R1M tumor–bearing athymic mice were injected with 37 MBq of the tracer. At 1, 6.5, 16, 19, 21, 24, and 31 h after injection, a 15-min static image was acquired (1,024 × 1,024 matrix; field of view of 23.5 × 12.46 cm; photopeak window set at 15% around 159 keV). The tumor retention of the tracer was calculated relative to the time point 1 h after injection. The tumor contrast was defined as DUR relative to the 1-h time point: relative DUR = percent injected activity per tumor pixel divided by percent injected activity per total pixels at 1, 6.5, 16, 19, 21, 24, or 24 h; the result was divided by DUR at steady state (1 h).

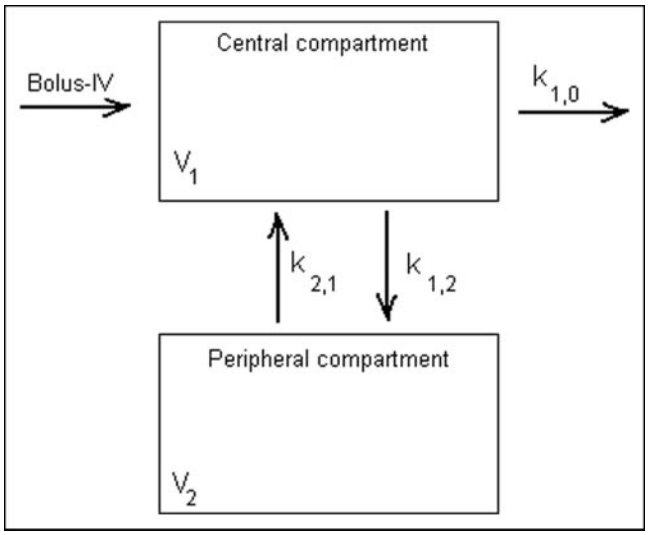

FIGURE 1. Graphic presentation of 2-compartment model applied to blood DPI data for ^{123}I-2-iodo-D-phenylalanine. IV = intravenous; V_2 = apparent distribution volume for peripheral compartment.

Dissection Analysis of Biodistribution of ^{123}I-2-Iodo-D-Phenylalanine in Tumor Model. The injected dose was calculated as described previously (*3*). The same mouse population as that used for the DPI experiments was used for these experiments. Thirty R1M tumor–bearing athymic mice were injected with 7.4 kBq of ^{123}I-2-iodo-D-phenylalanine 6 d after the last imaging experiment was performed. At various time points (2, 5, 10, 15, 30, 45, 60, 90, 120, and 180 min) after injection, 3 animals per time point were sacrificed. The amount of radioactivity in the organs and tissues was calculated as the differential absorption rate (DAR): (activity in tissue × total body weight)/(weight in tissue × activity in injected dose) (*3*).

Two-Compartment Modeling. The data obtained by DPI and dissection for ^{123}I-2-iodo-D-phenylalanine were fit to a 2-compartment model with intravenous bolus injection, without a lag time, and with first-order elimination by use of WinNonlin 4.0.1 (Pharsight Corp.) (Fig. 1). This kinetic model was chosen by analogy with ^{123}I-3-iodo-α-methyltyrosine (*10*) The primary parameters V_1 (apparent volume of distribution of the central compartment), $k_{1,0}$ (velocity of elimination from the central compartment), $k_{1,2}$ (velocity of distribution from the central compartment to the peripheral compartment), and $k_{2,1}$ (velocity of distribution from the peripheral compartment to the central compartment) were determined. To obtain the primary parameters for ^{123}I-2-iodo-L-phenylalanine, data from earlier work were used for the calculations (*3*).

Dissection Analysis of Biodistribution of ^{125}I-2-Iodo-D-Phenylalanine in Inflammation Model. Inflammation-bearing NMRI mice (n = 5) were injected with 7.4 kBq of ^{125}I-2-iodo-D-phenylalanine together with 16 MBq of ^{18}F-FDG at 24 h after turpentine injection. After 30 min, the mice were sacrificed, and the amount of radioactivity in the organs and tissues was calculated as the DAR (*3*).

Metabolism Study of In Vivo Stability of ^{125}I-2-Iodo-D-Phenylalanine. The blood collected in the dissection study was used for a metabolism study of ^{125}I-2-iodo-D-phenylalanine as a function of time as described previously (*3*).

Dosimetric Calculations

Mean time–activity curves, expressed as percent injected activity per weight of tissue (%IA/weight$_{tissue}$) or percent injected activity of tissue (%IA$_{tissue}$), were generated for the organs of interest from the dissection experiments. Source organ residence times were determined from time integration of the biexponential fit to the experimental biodistribution data. Fitting was performed with the SPSS 12.0 software package (SPSS Inc.). In order to fit the experimental data, 2 extra time points were generated, at 792 min and 2,376 min after injection (1 and 3 times the half-life of ^{123}I, respectively), by considering only the physical decay of the tracer and thus assuming the worst-case scenario. The latter procedure was performed because dissection was conducted only until 180 min after injection of the tracer. Extrapolation of the animal biodistribution to the reference human adult biodistribution was performed by assuming that either the %IA/weight$_{tissue}$ or the %IA$_{tissue}$ values were equal in mice and humans. Absorbed radiation dose estimates then were calculated for the target organs by applying MIRD methodology (*11*) for healthy adults with the MIRDOSE3.0 software package (MIRD Committee, Society of Nuclear Medicine, Reston, VA). The absorbed dose estimate for the urine bladder wall was calculated by use of the dynamic bladder model with a bladder voiding interval of 4.8 h as described by Cloutier et al. (*12*). The dosimetric calculations were performed not only on the data mentioned in this article but also on previously reported dissection data for 2-iodo-L-phenylalanine and 2-iodo-L-tyrosine to compare the new D-isomer tracer to other, newly developed amino acid analogs (*3,13*).

The parameters of the exponential fitted curves in SPSS were applied for hierarchical clustering of the organs by use of the average linkage algorithm. This analysis was performed to discover which organs exhibit the same behavior for ^{123}I-2-iodo-D-phenylalanine tracer biodistribution.

RESULTS

Synthesis and Radiolabeling of 2-Iodo-D-Phenylalanine

Yields of up to 65% were obtained for the precursor synthesis of 2-iodo-D-phenylalanine from 2-bromo-D-phenylalanine by the Cu^{1+}-assisted nucleophilic exchange method.

Radioiodination of 2-iodo-D-phenylalanine by Cu^{1+}-assisted isotopic exchange, followed by Ag membrane filtration, resulted in a radiochemical purity of >99% and specific activities of 65 GBq/mmol (^{123}I labeling) and 11 GBq/mmol (^{125}I labeling).

In both cases, it was shown by chiral HPLC that there was no detectable amount of L-isomer analogs.

In Vivo Results

In Vivo Stability of ^{125}I-2-Iodo-D-Phenylalanine. HPLC analysis of mouse blood showed 4.8% free iodide at 90 min after injection. No other metabolites were detected. Ethylenediaminetetraacetic acid did not have any influence on the deiodination of ^{125}I-2-iodo-D-phenylalanine.

DPI. DPI with ^{123}I-iodo-HSA revealed no significant difference between blood flow in the tumor and blood flow in the reference contralateral leg: RTB = 1.1 ± 0.2 (mean ± SD).

At equilibrium (plateau phase), net ^{123}I-2-iodo-D-phenylalanine uptake in the tumor was high. An overall mean

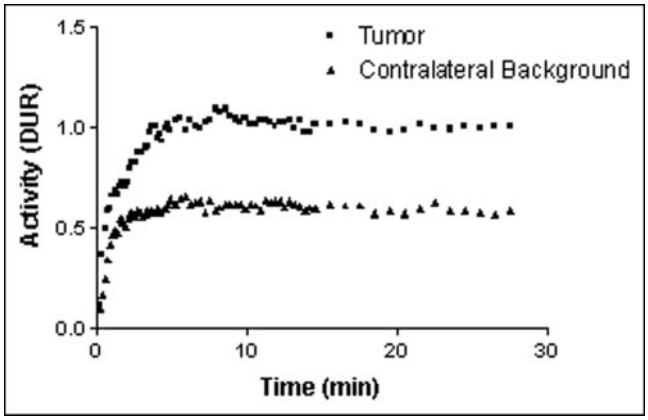

FIGURE 2. Overall mean ^{123}I-2-iodo-D-phenylalanine uptake (DUR) in tumor and contralateral background region as function of time, as determined by DPI (n = 30).

^{123}I-2-iodo-D-phenylalanine uptake by tumors of 1.00 ± 0.02 was obtained (Fig. 2). The administration of L-phenylalanine resulted in a significant displacement of the ^{123}I-2-iodo-D-phenylalanine activity from the tumor; the radioactivity in the tumor showed a decrease of 9.6% ± 2.3% from the initial uptake value ($P < 0.05$) after the intravenous administration of L-phenylalanine.

^{123}I-2-Iodo-D-phenylalanine elimination from blood showed renal clearance to the bladder (Fig. 3). High tracer uptake was noted in the zone of the pancreas; it reached a peak value of 3.3 ± 0.2 at 2 min after injection but decreased rapidly (Fig. 4). Because of superposition of the pancreas with other organs, such as the left kidney and the stomach, the results of uptake in the pancreas are overestimated (*14*). Low uptake of radioactivity was observed in the

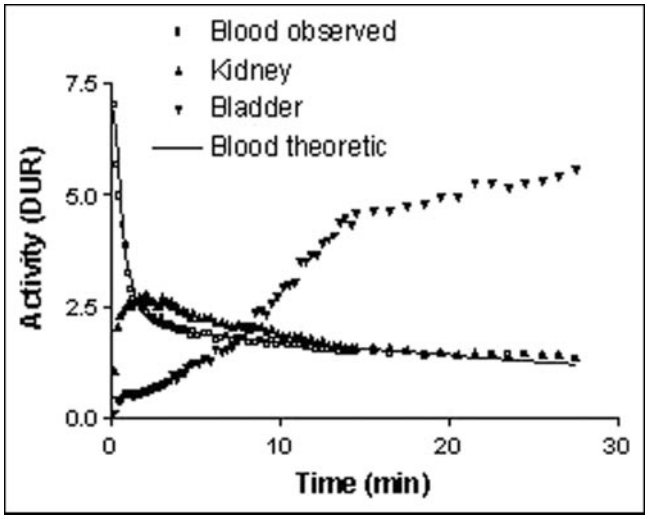

FIGURE 3. Uptake of ^{123}I-2-iodo-D-phenylalanine (DUR) as function of time, as determined by DPI, and clearance of tracer through kidneys to bladder. Kinetic fitting of observed blood curve for ^{123}I-2-iodo-D-phenylalanine tracer distribution with theoretic curve (solid line) was done with 2-compartment model (n = 30).

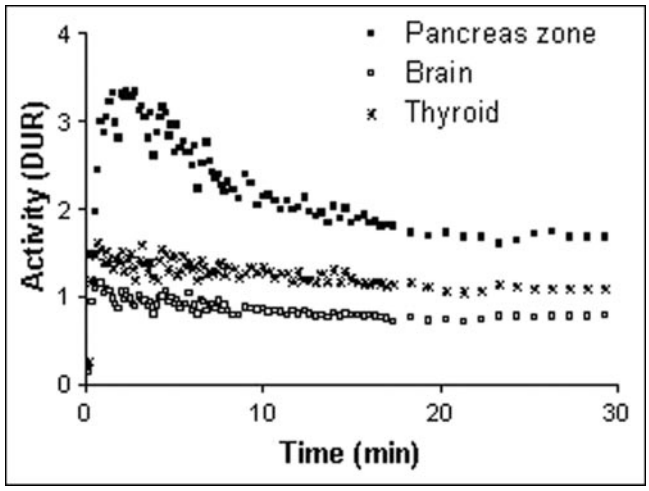

FIGURE 4. Uptake of ^{123}I-2-iodo-D-phenylalanine (DUR) in pancreatic zone, brain, and thyroid (n = 30).

thyroid (1.08 ± 0.06) and in the brain (0.76 ± 0.05) (Fig. 4).

The retention study for ^{123}I-2-iodo-D-phenylalanine showed that only 4% of the initial ^{123}I-2-iodo-D-phenylalanine uptake remained in the tumor at 31 h after injection. However, when tumor contrast was evaluated, an increase of 352% at 19 h after injection was observed (Table 1).

Dissection Analysis of Biodistribution. Biodistribution data for ^{125}I-2-iodo-D-phenylalanine at 2, 30, 60, and 120 min after injection in R1M tumor–bearing athymic mice are shown in Table 2. Those for ^{125}I-2-iodo-L-phenylalanine were reported previously (*3*).

The net ^{125}I-2-iodo-D-phenylalanine uptake by tumors reached equilibrium at 30 min with a mean ± SD DAR of 3.9 ± 1.2. At the same time point, ^{125}I-2-iodo-D-phenylalanine activity in blood and in the contralateral leg tissue reached DARs of 1.3 ± 0.2 and 1.1 ± 0.2, respectively.

TABLE 1
Retention of ^{123}I-2-Iodo-D-Phenylalanine Activity in Tumors, as Determined by Planar γ-Scintigraphy (n = 3)

Time (h)	Tumor contrast (mean ± SD %)*		Tumor retention (mean ± SD %)†	
	2-I-L-Phe	2-I-D-Phe	2-I-L-Phe	2-I-D-Phe
1	100 ± 0	100 ± 0	100.0 ± 0.0	100.0 ± 0.0
6.5	100 ± 2	120 ± 22	67.8 ± 2.5	52.6 ± 10.7
16	75 ± 19	314 ± 36	23.2 ± 5.6	15.5 ± 1.6
19	71 ± 17	352 ± 31	23.1 ± 7.9	6.7 ± 2.1
21	95 ± 25	213 ± 34	21.1 ± 8.5	5.0 ± 1.7
24	91 ± 16	251 ± 36	17.1 ± 6.3	5.0 ± 2.0
31	86 ± 16	197 ± 10	11.6 ± 3.9	4.0 ± 1.1

*Percent contrast enhancement in comparison with initial ^{123}I-2-iodo-L-phenylalanine (2-I-L-Phe) or ^{123}I-2-iodo-D-phenylalanine (2-I-D-Phe) tumor contrast.

†Percentage of initial ^{123}I-2-iodo-L-phenylalanine or ^{123}I-2-iodo-D-phenylalanine uptake that remained in tumors.

TABLE 2
Biodistribution Analysis by Dissection of ^{125}I-2-Iodo-D-Phenylalanine in R1M Tumor–Bearing Athymic Mice (n = 3)

Sample	Mean ± SD DAR at following time (min):			
	2	30	60	120
Blood	3.10 ± 0.12	1.25 ± 0.21	1.08 ± 0.12	1.06 ± 0.05
Brain	0.33 ± 0.07	0.36 ± 0.06	0.42 ± 0.05	0.38 ± 0.10
Heart	2.13 ± 0.07	1.04 ± 0.29	0.81 ± 0.10	0.73 ± 0.04
Lungs	2.17 ± 0.12	0.91 ± 0.20	0.75 ± 0.07	0.71 ± 0.09
Stomach	0.68 ± 0.20	1.87 ± 1.13	2.14 ± 1.15	2.83 ± 1.75
Spleen	2.20 ± 0.28	0.99 ± 0.28	0.81 ± 0.20	0.95 ± 0.12
Liver	2.21 ± 0.23	0.91 ± 0.16	1.02 ± 0.25	1.07 ± 0.33
Kidneys	17.65 ± 2.55	6.88 ± 3.27	2.97 ± 0.24	2.05 ± 0.04
Small intestine	1.33 ± 0.13	1.02 ± 0.31	1.20 ± 0.14	1.88 ± 0.71
Large intestine	0.64 ± 0.07	0.40 ± 0.20	0.50 ± 0.11	1.73 ± 0.20
Fatty tissue	0.73 ± 0.39	0.66 ± 0.45	0.19 ± 0.02	0.32 ± 0.10
Contralateral background	1.10 ± 0.21	1.06 ± 0.19	0.68 ± 0.12	0.66 ± 0.04
Pancreas	10.52 ± 3.63	10.68 ± 5.18	6.84 ± 1.07	6.17 ± 0.53
Tumor	2.05 ± 0.82	3.89 ± 1.22	2.30 ± 0.39	2.09 ± 0.54
RTB	1.86 ± 0.36	3.64 ± 0.48	3.38 ± 0.52	3.13 ± 0.73

^{125}I-2-Iodo-D-phenylalanine was cleared very fast through the kidneys, without accumulation. High uptake of radioactivity was observed in the pancreas. Very low accumulation of radioactivity was observed in other abdominal organs, such as the liver, small intestine, and large intestine, the lungs, or the brain.

Comparison of ^{18}F-FDG uptake with ^{125}I-2-iodo-D-phenylalanine uptake at the inflammation site resulted in ratios for inflamed muscle to contralateral muscle of 10.5 ± 2.1 and 1.43 ± 0.09, respectively.

Two-Compartment Modeling. The results obtained by 2-compartment modeling are shown in Figure 4 and Table 3. They showed that ^{123}I-2-iodo-D-phenylalanine biodistribution analyzed by DPI and dissection fitted the theoretic curve for the proposed kinetic model (all R^2 values were >0.95). In comparison with its L-isomer, ^{123}I-2-iodo-D-phenylalanine was cleared from blood almost 2 times faster. Moreover, ^{123}I-2-iodo-D-phenylalanine was taken up in the peripheral compartment faster, but its velocity of elimination from this compartment was comparable to that of ^{123}I-2-iodo-L-phenylalanine. Both biodistribution methods showed the same kinetic patterns.

Dosimetry

Mean radiation dose estimates were calculated for the reference human adult by use of time–activity curves and organ residence times derived from mouse biodistribution data. The MIRDOSE3.0 program was applied, assuming that the values for either the percent injected activity per gram (%IA/g) of tissue or the percent injected activity (%IA) for ^{123}I-2-iodo-D-phenylalanine, ^{123}I-2-iodo-L-phenylalanine, and ^{123}I-2-iodo-L-tyrosine in mice are equal to those in humans. Dosimetry results obtained from both estimates are summarized in Table 4. They show that the highest equivalent organ doses were reached for the pancreas and the stomach. For selection of the highest equivalent organ dose for each organ by both dosimetry estimates, this worst-case scenario would result in effective doses of 0.0330, 0.0375, and 0.0542 mSv/MBq for ^{123}I-2-iodo-D-phenylalanine, ^{123}I-2-iodo-L-phenylalanine, and ^{123}I-2-iodo-

TABLE 3
Kinetic Parameters of 2-Compartment Model Applied to Blood DPI Data for ^{123}I-2-Iodo-D-Phenylalanine and ^{123}I-2-Iodo-L-Phenylalanine

Parameter	Unit	Mean ± SD for:					
		2-Iodo-D-phenylalanine		2-Iodo-L-phenylalanine		D/L Ratio*	
		DPI results	Dissection results	DPI results	Dissection results	DPI results	Dissection results
V_1	$Activity_{total}$/DUR†	7.10 ± 0.10	6.68 ± 0.18	9.65 ± 0.20	18.78 ± 0.62	0.74 ± 0.02	0.35 ± 0.02
$k_{1,0}$	1/min	0.075 ± 0.004	0.0025 ± 0.0003	0.035 ± 0.003	0.0014 ± 0.0002	2.14 ± 0.23	1.79 ± 0.33
$k_{1,2}$	1/min	1.09 ± 0.04	0.060 ± 0.010	0.80 ± 0.04	0.009 ± 0.003	1.36 ± 0.08	6.67 ± 4.00
$k_{2,1}$	1/min	0.41 ± 0.01	0.030 ± 0.06	0.42 ± 0.02	0.019 ± 0.007	0.98 ± 0.05	1.58 ± 0.33

*Ratio for ^{123}I-2-iodo-D-phenylalanine to ^{123}I-2-iodo-L-phenylalanine.
†$Activity_{total}$/DUR = total amount of activity injected/differential uptake ratio.

TABLE 4
Dosimetric Calculations and Estimation of Worst-Case Effective Doses for ^{123}I-2-Iodo-D-Phenylalanine, ^{123}I-2-Iodo-L-Phenylalanine, and ^{123}I-2-Iodo-L-Tyrosine (n = 3)*

Organ	2-Iodo-D-phenylalanine		2-Iodo-L-phenylalanine		2-Iodo-L-tyrosine	
	Dose %IA	Dose %IA/g	Dose %IA	Dose %IA/g	Dose %IA	Dose %IA/g
Adrenal glands	1.56E−02	9.24E−03	1.39E−02	1.04E−02	2.38E−02	1.26E−02
Brain	4.95E−03	5.18E−03	4.37E−03	6.37E−03	1.14E−02	1.30E−02
Breasts	6.23E−03	5.59E−03	5.95E−03	6.46E−03	6.07E−03	6.26E−03
Gallbladder wall	1.78E−02	9.61E−03	1.52E−02	1.09E−02	2.66E−02	1.33E−02
LLI wall	2.46E−02	8.98E−03	2.85E−02	2.02E−02	4.92E−02	1.94E−02
Small intestine	3.41E−02	1.15E−02	2.59E−02	1.42E−02	4.02E−02	1.48E−02
Stomach	1.28E−01	1.92E−02	5.49E−02	1.30E−02	5.83E−02	1.36E−02
ULI wall	2.88E−02	9.20E−03	2.21E−02	1.16E−02	4.55E−02	1.28E−02
Heart wall	1.32E−02	1.01E−02	1.05E−02	9.36E−03	1.81E−02	1.49E−02
Kidneys	2.07E−02	8.02E−03	9.07E−03	6.00E−03	5.20E−02	1.84E−02
Liver	1.69E−02	8.29E−03	1.24E−02	6.92E−03	3.64E−02	1.62E−02
Lungs	8.89E−03	9.44E−03	6.99E−03	8.08E−03	1.18E−02	1.49E−02
Muscle	8.94E−03	7.00E−03	1.07E−02	1.06E−02	1.14E−02	9.92E−03
Ovaries	1.51E−02	9.34E−03	2.19E−02	2.00E−02	2.50E−02	1.80E−02
Pancreas	1.98E−01	4.27E−02	2.14E−01	4.91E−02	5.41E−01	1.24E−01
Red marrow	8.77E−03	6.87E−03	9.35E−03	9.28E−03	1.07E−02	8.91E−03
Bone surfaces	1.47E−02	1.28E−02	1.56E−02	1.65E−02	1.65E−02	1.57E−02
Skin	5.49E−03	4.92E−03	6.03E−03	6.53E−03	5.84E−03	5.95E−03
Spleen	2.32E−02	8.90E−03	2.37E−02	1.03E−02	3.93E−02	1.40E−02
Testes	6.85E−03	6.63E−03	1.36E−02	1.46E−02	1.19E−02	1.26E−02
Thymus	7.93E−03	7.50E−03	7.77E−03	8.68E−03	7.72E−03	8.36E−03
Thyroid	7.44E−03	7.42E−03	7.60E−03	8.85E−03	6.79E−03	8.00E−03
Urine bladder wall	9.93E−03	9.29E−03	3.02E−01	3.03E−01	2.61E−01	2.60E−01
Uterus	1.33E−02	9.40E−03	3.64E−02	3.55E−02	3.49E−02	3.12E−02
Total body	1.03E−02	7.50E−03	1.14E−02	1.09E−02	1.38E−02	1.08E−02
Worst-case dose (mSv/MBq)	3.30E−02		3.75E−02		5.42E−02	

*Doses are expressed as mGy/MBq, unless otherwise indicated. Calculations for dose %IA and dose %AI/g were performed assuming that values for either %IA/weight$_{tissue}$ or %IA$_{tissue}$ were equal in mice and humans.
LLI = lower large intestine; ULI = upper large intestine.

L-tyrosine, respectively. Although no statistically significant difference was observed between the 2 phenylalanine analogs (P = 0.378), the tyrosine analog differed significantly from the other tracers (P = 0.041).

The clustering results for the coefficients of the exponential models used in the dosimetric calculations are visually presented by the dendrogram in Figure 5. It shows the closeness of the different organs with respect to ^{123}I-2-iodo-D-phenylalanine pharmacokinetic behavior. The dendrograms for ^{123}I-2-iodo-L-phenylalanine and ^{123}I-2-iodo-L-tyrosine are not shown, but they demonstrated the same behavior. It is clear that the tumor, the remainder of the body, the kidneys, and the stomach are separate groups, with 2 additional clusters: blood group (blood, lungs, spleen, heart, and liver) and other-organ group (brain, large and small intestines, pancreas, and bladder). When the elimination coefficients only are examined (dendrogram not shown), an identical, even more pronounced, pattern was observed, with the exception of the stomach, which belonged to the blood group. Indeed, the kinetics of elimina-

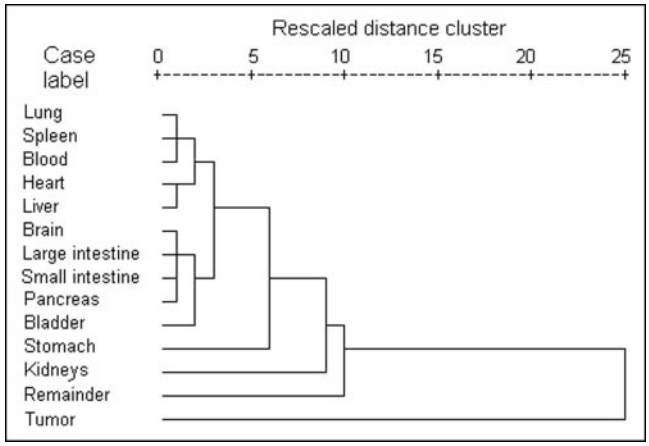

FIGURE 5. Hierarchical clustering with average linkage algorithm for exponential curve parameters obtained by nonlinear regression of dissection data for 2-iodo-D-phenylalanine.

tion from the stomach were similar to those for the blood group organs which, however, did not show uptake kinetics under the experimental conditions applied. These clustering results indicate that not every organ should be considered separately in full pharmacokinetic modeling because of similar pharmacokinetic behaviors within the groups.

DISCUSSION

Tamemasa et al. reported the preferential uptake of D-amino acids in tumor-bearing mice (*4,5*). Moreover, Yanagida et al. showed in tumor cells in vitro that the LAT transporter seems to lack stereospecificity; D-amino acids are transported with a high affinity by LAT1 (*2*). Because of the successful results obtained with ^{125}I-2-iodo-L-phenylalanine, ^{125}I-2-iodo-D-phenylalanine was developed, and its tumor-detecting characteristics were evaluated.

In vitro in R1M cells, the Michaelis–Menten constant (K_m) values for ^{125}I-2-iodo-D-phenylalanine, ^{125}I-2-iodo-L-phenylalanine, and the natural amino acid L-phenylalanine were similar. All compounds were transported by the same obligatory exchange system, LAT1 (*6*), confirming the hypothesis made by Yanagida et al. (*2*). In vitro (full minimal essential medium buffer), the accumulation of ^{125}I-2-iodo-D-phenylalanine in R1M cells over a longer period of time (up to 24 h) was noted, although no incorporation into cell proteins was found, just as with the L-isomer (*2,15*).

Given the above-mentioned characteristics, the new tracer ^{123}I-2-iodo-D-phenylalanine was evaluated in vivo for its potential application for oncologic diagnostic imaging by DPI.

Like 2-iodo-L-phenylalanine, the D-isomer could be synthesized easily and radioiodinated quantitatively with a kit formulation by use of Cu^{1+}-assisted nucleophilic exchange (*3*). The same precursor yields and the same tracer specific activities were obtained for both tracers. No metabolism of ^{125}I-2-iodo-D-phenylalanine took place. Only minor dehalogenation was observed; this dehalogenation was somewhat lower that that of the L-isomer and was reflected by the low radioactivity uptake in the thyroid. Thus, oral administration of stable potassium iodide before injection of ^{123}I-2-iodo-D-phenylalanine should protect the thyroid from radioiodine poisoning.

Concerning the DPI data for ^{123}I-2-iodo-D-phenylalanine, tracer kinetics were in accordance with the proposed 2-compartment model. Moreover, because of its higher $k_{1,0}$ value and thus faster elimination from blood, 2-iodo-D-phenylalanine will demonstrate better tumor contrast at the same time point than its L-isomer. Additionally, 2-iodo-D-phenylalanine was taken up by the peripheral compartment faster than 2-iodo-L-phenylalanine ($k_{1,2}$ for the D-isomer $\approx$ 1.4 times $k_{1,2}$ for the L-isomer), but both tracers were eliminated at equal velocities from the peripheral compartment ($k_{2,1}$ for the D-isomer $\approx$ $k_{2,1}$ for the L-isomer). These findings, together with the very fast ^{123}I-2-iodo-D-phenylalanine washout from the pancreas, will lead to faster and higher tumor uptake and thus better tumor contrast for ^{123}I-2-iodo-D-phenylalanine than for the L-analog. This hypothesis was confirmed by the results of the ^{123}I-2-iodo-D-phenylalanine tumor retention study. Although only 4% of the initial ^{123}I-2-iodo-D-phenylalanine uptake remained in the tumor after 31 h, the tumor contrast became much more favorable for oncologic imaging than that obtained with ^{123}I-2-iodo-L-phenylalanine, with a retention of 11%; whereas the latter showed a decrease in tumor contrast, ^{123}I-2-iodo-D-phenylalanine showed an increase in contrast of 352% at 19 h after injection (Table 1). These results demonstrate the capability of 2-iodo-D-phenylalanine as a tumor-detecting agent in SPECT and indicate the potential of 2-iodo-D-phenylalanine as a radiotherapeutic agent. Indeed, metaiodobenzylguanidine, which showed tumor uptake of only 2% of the injected dose, has become an effective antineuroblastoma agent, in addition to its diagnostic tumor imaging application. Apart from its tumor-targeting properties, the new tracer 2-iodo-D-phenylalanine is metabolically stable but shows lower liver uptake and accumulation than metaiodobenzylguanidine and is rapidly cleared from the circulation by the kidneys; these properties are ideal starting points for systemic radiotherapy (*16–18*).

Different absolute values were obtained when data from DPI and data from dissection were used, but the same kinetic trends were observed. Indeed, this finding is emphasized by the ratio ^{123}I-2-iodo-D-phenylalanine to its L-isomer in Figure 1.

Although the kinetic modeling of both tracers showed similar trends for DPI and dissection, the values differed significantly from each other. This finding could be explained by the difference in data acquisition; the ROI for blood in DPI also includes the heart muscle. Although the dissection results showed that no accumulation of the tracer took place in the heart muscle (primary energy source: glucose), the latter tissue could have an additional effect on the total counts in the ROI, resulting in higher values.

Regarding tumor uptake, DPI showed that ^{123}I-2-iodo-D-phenylalanine accumulated quickly to reach a high level in R1M tumors. The specificity of this ^{123}I-2-iodo-D-phenylalanine uptake by tumors was confirmed by the small contribution of blood flow to tumor activity, by the small but significant amount of radioactivity displaced by L-phenylalanine coupled to the obligatory exchange by LAT1, and by the minor uptake in inflamed tissue.

Moreover, low abdominal background activity, fast clearance from blood, and low uptake in the brain were observed (Figs. 3 and 4; Table 2); these findings are favorable for brain tumor detection as well as peripheral tumor detection. Compared with those for 2-iodo-L-phenylalanine, the net tumor uptake and RTB for 2-iodo-D-phenylalanine were similar, but the D-isomer was cleared from blood 2 times faster (Figs. 1 and 3) (*3*). The latter properties will result in better ratios of uptake in tumors to uptake in blood and less radiation burden to the animal.

Exogenous uptake of D-amino acids (by ingestion or from microorganisms) will lead to metabolism by D-amino acid oxidase, present in the liver, kidneys, and pancreas paren-

chyma. The latter, together with the stereospecificity of the translational machinery, will result in the formation of proteins uniquely consisting of L-amino acids (*10,19*). Although 2-iodo-D-phenylalanine showed high uptake in the pancreatic zone, it was excreted very fast. This observation could imply that the D-isomer, just like ^{123}I-2-iodo-L-phenylalanine, is not incorporated into cell proteins, because the pancreas in rodents demonstrates high protein turnover. In humans, high uptake of radiolabeled amino acids in the pancreas does not occur (*10*).

The above-mentioned characteristics of ^{123}I-2-iodo-D-phenylalanine make this tracer a potential diagnostic tool for oncologic imaging. The rapid clearance from blood, together with the high, fast, and specific tumor uptake, should lead to specific targeting of the tumor with minor radiation burden to other organs and tissues, leading to the possible therapeutic application of this tracer.

Relative to the DPI study, the dissection study presented more detailed, but similar, results regarding tracer distribution. It confirmed the high tumor uptake but the low abdominal uptake of ^{123}I-2-iodo-D-phenylalanine and its renal clearance. Regarding dosimetry, important differences among the 3 amino acid analogs were observed; of the 3 tracers, 2-iodo-L-tyrosine showed the highest effective dose, but 2-iodo-L-phenylalanine and 2-iodo-D-phenylalanine showed comparable doses. Moreover, accumulation in the pancreas is typical in rodents but does not appear in humans, a property that will additionally lead to lower effective doses (e.g., 2.61×10^{-2} for the D-analog). All 3 amino acid analogs showed a favorable biodistribution for a tumor imaging agent. The effective dose will lead to a radiation dose that is comparable to those used in other diagnostic nuclear medicine procedures if the trend seen in the mouse model is seen in humans. Indeed, administration of the compounds to healthy volunteers in a study of human biodistribution will result in an effective dose of less than 1 mSv, the limit for category IIb studies (*20*).

By use of the hierarchical classification of the organs with the experimental fitted kinetic parameters obtained for ^{123}I-2-iodo-D-phenylalanine, ^{123}I-2-iodo-L-phenylalanine, and ^{123}I-2-iodo-L-tyrosine, a first step toward physiologic modeling could be undertaken. This analysis indicated that not every organ should be considered separately in full pharmacokinetic modeling because of similar pharmacokinetic behaviors within the groups. Five different groups could be defined: tumor, remainder of the body, stomach, blood group, and other-organ group. The stomach as an individual group could be explained by the uptake of free $^{123}I^-$ after dehalogenation.

The above-mentioned characteristics of ^{123}I-2-iodo-D-phenylalanine make this tracer a potential diagnostic tool for oncologic imaging, similar to the L-analog but with the potential for therapeutic application. The rapid clearance from blood, together with the high, fast, and specific tumor uptake, should lead to specific targeting of the tumor with minor radiation burden to other organs and tissues.

CONCLUSION

^{123}I-2-Iodo-D-phenylalanine is a promising tracer for diagnostic oncologic imaging because of its high, fast, and specific tumor uptake and fast clearance from blood. Moreover, the new tracer possesses better diagnostic imaging characteristics regarding enhanced tumor contrast than its L-analog.

REFERENCES

1. Jager PL, Vaalburg W, Pruim J, et al. Radiolabeled amino acids: basic aspects and clinical applications in oncology. *J Nucl Med*. 2001;42:432–445.
2. Yanagida O, Kanai Y, Chairoungdua A, et al. Human L-type amino acid transport system 1 (LAT1): characterisation of function and expression in tumor cell lines. *Biochim Biophys Acta*. 2001;1514:291–302.
3. Kersemans V, Cornelissen B, Kersemans K, et al. In vivo characterization of ^{123}I/^{125}I-2-iodo-L-phenylalanine in an R1M rhabdomyosarcoma athymic mouse model as a potential tumor tracer for SPECT. *J Nucl Med*. 2005;46:532–539.
4. Tamemasa O, Goto R, Suzuki T. Preferential incorporation of some ^{11}C-labeled D-amino acids into tumor bearing animals. *Gann*. 1978;69:517–523.
5. Tamemasa O, Goto R, Taketa A, et al. High uptake of ^{11}C-labelled D-amino acids by various tumors. *Gann*. 1982;73:147–152.
6. Mertens JJR, Kersemans V, Lahoutte T, et al. Radioiodo-D-2-I-phenylalanine: a new tumor specific tracer for diagnosis and systemic radionuclide therapy [abstract]. *Eur J Nucl Med*. 2004;31(suppl):S220.
7. Waterton JC, Alott CP, Pickfort R, et al. Assessment of mouse tumor xenograft volumes in vivo by ultrasound imaging, MRI and calliper measurement. In: Faulkner K, Carey B, Crellin A, Harisson RM, eds. *Proceedings of the 19th LH Gray Conference*: *Quantitative Imaging in Oncology*. London, U.K.: Kluwer Academic Publishers; 1997:146–149.
8. Boellaard R, Krak NC, Hoekstra OS, Lammertsma AA. Effects of noise, image resolution, and ROI definition on the accuracy of standard uptake values: a simulation study. *J Nucl Med*. 2004;45:1519–1527.
9. Thie JA. Understanding the standardized uptake value, its methods, and implications for usage. *J Nucl Med*. 2004;45:1431–1434.
10. Langen KJ, Pauleit D, Coenen HH, et al. 3-[^{123}I]Iodo-alpha-methyl-L-tyrosine: uptake mechanisms and clinical applications. *Nucl Med Biol*. 2002;29:625–631.
11. Loevinger R, Budinger T, Watson E. *MIRD Primer for Absorbed Dose Calculations*. New York, NY: Society of Nuclear Medicine; 1991:1–17.
12. Cloutier RJ, Smith SA, Watson EE, Snyder WS, Warner GG. Dose to the fetus from radionuclides in the bladder. *Health Phys*. 1973;25:147–161.
13. Kersemans V, Kersemans K, Cornelissen B, et al. Comparison of the new tumor tracer ^{123}I-2-iodo-L-phenylalanine with ^{123}I-2-iodo-L-tyrosine [abstract]. *J Nucl Med*. 2005;46(suppl):355P.
14. Cook MJ. *The Anatomy of the Laboratory Mouse*. New York, NY: Academic Press; 1965:55–78.
15. Mertens J, Kersemans V, Bauwens M, et al. Synthesis, radiosynthesis, and in vitro characterization of [^{125}I]-2-iodo-L-phenylalanine in a R1M rhabdomyosarcoma cell model as a new potential tumor tracer for SPECT. *Nucl Med Biol*. 2004;31:739–746.
16. Rutgers M, Buitenhuis CKM, Hoefnagel CA, et al. Targeting of meta-iodobenzylguanidine to SK-N-SH human neuroblastoma xenografts: tissue distribution, metabolism and therapeutic efficacy. *Int J Cancer*. 2000;87:412–422.
17. Hoefnagel CA, Lewington VJ. MIBG therapy. In: Murray IPC, Ell PJ, eds. *Nuclear Medicine in Clinical Diagnosis and Treatment*. 2nd ed. London, U.K.: Churchill Livingstone; 1998:1067–1081.
18. Matthay KK, Desantes K, Hasegawa B, et al. Phase I dose escalation of ^{131}I-metaiodobenzylguanidine with autologous bone marrow support in refractory neuroblastoma. *J Clin Oncol*. 1998;16:229–236.
19. Yang H, Zheng G, Peng X, et al. D-Amino acids and D-Tyr-tRNA^{Tyr} deacylase: stereospecificity of the translation machine revisited. *FEBS Lett*. 2003;552:95–98.
20. Beekhuis H. Population radiation absorbed dose from nuclear medicine procedures in the Netherlands. *Health Phys*. 1988;54:287–291.